

# Ultrasonic Diagnostic System for Interactive Interrogation of Adult Brain Through Intact Skull

F. J. FRY,\* N. T. SANGHVI,\* R. F. MORRIS,\* J. L. CLENDENON,\*  
K. A. DINES,\* J. T. PATRICK,† AND S. A. GOSS\*

Fry FJ, Sanghvi NT, Morris RF, Clendenon JL, Dines KA, Patrick JT, Goss SA. Ultrasonic diagnostic system for interactive interrogation of adult brain through intact skull. *Invest Radiol* 1982;17:463-469.

An integrated ultrasonic system has been developed employing static gray scale imaging, digital image processing, and analyses of quantitative ultrasonic backscatter for interactive interrogation of brain through the adult human skull. Operating at 750 kHz, to avoid severe spatial and temporal pulse distortion which accompany ultrasonic transskull transmission at higher frequencies, storage and image processing of successive images taken at selected gain settings in the same image plane allow the reconstruction of a composite cross-section of the brain and skull and enable visualization of internal brain structure. Analysis of digitized backscatter data obtained with the visualization transducer over selectable interrogation paths referenced to the cross-sectional image permit quantitative classification of tissue type independent of qualitative visual image analysis, such that enhanced diagnostic potential is provided. A previous paper<sup>1</sup> described in detail the modifications of the commercial ultrasound diagnostic unit which serves as the core of this system. The present paper presents the rationale for the integrated system design approach, as well as a description of graphics display and tissue classification features which have been incorporated into the instrumentation configuration and are deemed necessary for successful transskull ultrasonic imaging and diagnosis.

**Key words:** ultrasound, imaging, brain, skull.

From the \*Indianapolis Center for Advanced Research, Inc., Indianapolis, Indiana, and the †Division of Neurosurgery, Indiana University School of Medicine, Indianapolis, Indiana.

The authors acknowledge the partial support of this work by the National Institutes of Health (Research Grant No. 5R01NS14201-02) and by the Indianapolis Center for Advanced Research, Inc.

The authors gratefully acknowledge the contributions of W. A. Erdmann, K. W. Johnston, M. Serrone, and H. W. White to the overall project, especially in the instrumentation design and construction phases of the work. Dr. R. F. Heimburger of the Division of Neurosurgery, Indiana University School of Medicine, provided the two patients selected for these preliminary studies.

Reprint requests: Stephen A. Goss, PhD, Indianapolis Center for Advanced Research, Life Science Research Division, Indiana University Hospital Rm A-32, 926 W. Michigan St., Indianapolis, Indiana 46223.

Received September 14, 1981, and accepted for publication April 8, 1982.

A NUMBER of studies over the last 30 years have sought ultrasonically to visualize the human brain through intact skull for medical diagnostic purposes, with varying degrees of success.<sup>2-9</sup> Few of the images produced by these early studies in adults, however, could be favorably compared with those obtained without intervening skull,<sup>10-12</sup> where essentially all soft tissue fluid interfaces (ventricles, sulci, fissures, cisterns, and blood vessels) could be detected. In addition, gray-white matter interfaces involving the internal capsule and the thalamus,<sup>13</sup> lesions produced by a variety of insults,<sup>14,15</sup> and hemorrhage have all been visualized ultrasonically, without the use of dyes or other image enhancement means.

The ability to visualize brain ultrasonically with this degree of success without intervening skull suggested that the technique was plausible if the interfering effects of the skull could be averted. Most of the past attempts at transskull imaging have been made at generally available diagnostic frequencies, usually 2.25 to 3.5 MHz. In more recent studies, frequencies in the range of 1 MHz have been implemented using a phased array of elements with dynamic focusing, beam sector sweeping, and array element transit time compensation for phase adjustment,<sup>16,17</sup> providing an increased transskull imaging capability.

Earlier reports from our laboratory have investigated the acoustic propagation properties of skull<sup>18</sup> and the degree to which focused ultrasound beams are distorted and displaced upon passage through skull<sup>19,20</sup> in an effort to better define those conditions favorable for minimal transskull transmission effects. Based upon these studies and those of Barger<sup>21</sup> in the classification of brain tissue using analyses of backscattered ultrasonic energy, a comprehensive diagnostic system has been developed which employs B-scan imaging, digital image processing, and quantitative analyses of ultrasonic backscatter for interactive interrogation of brain through the intact adult human skull. The present report describes the overall instrumentation design and

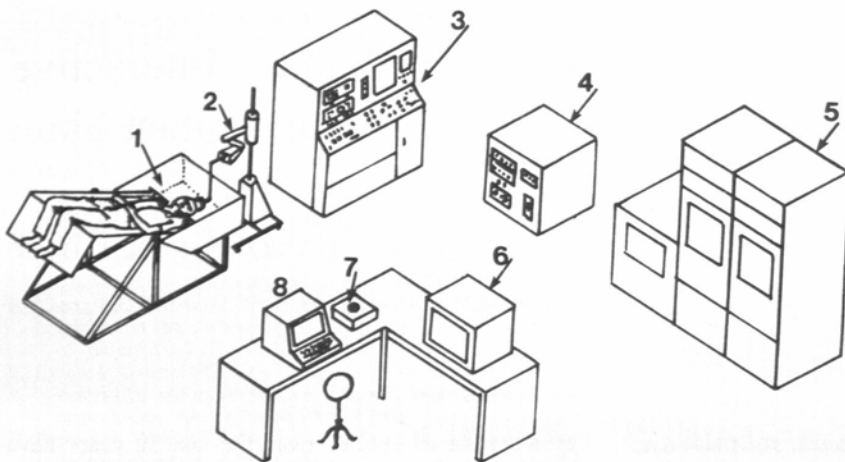


Fig. 1. Instrumentation configuration of ultrasonic transkull visualization system (UTIS): (1) patient scanning bath; (2) transducer scan arm (manual); (3) modified Searle Pho-Sonic<sup>®</sup> B-scan unit; (4) digital image controller; (5) PDP-11/45 digital computer with graphics display system and disk storage; (6) graphics monitor; (7) graphics trackball; (8) computer terminal.

capability and the rationale for the development of each subsystem.

### System Overview

The ultrasonic transkull interrogation system (UTIS) described herein has been designed to either circumvent or minimize the substantial effects introduced by the presence of skull in the sound path at typical diagnostic frequencies. In addition, the UTIS expands diagnostic capability from solely a qualitative interpretation of B-scan imaging to a quantitative diagnostic capability which acts synergistically with the visualization mode, providing new diagnostic information for the clinician. The overall system layout is depicted in Fig. 1.

The UTIS consists of four basic subsystems: (1) patient scanning; (2) low-frequency, modified B-scan instrumentation; (3) image processing and display hardware and software; and (4) tissue classification software. In order to minimize spatial and temporal distortion known to be substantial at higher frequencies,<sup>18-20</sup> the UTIS operates at 750 kHz. A highly modified commercial B-scan unit (Searle Pho-Sonic<sup>®</sup>) serves as the core of the system. The patient is scanned with the head partially immersed in a water bath to provide satisfactory acoustic coupling severely compromised by the presence of hair when other more convenient scanning regimes are employed. Composite images of skull and internal brain structure are produced by linearly combining images obtained under gain conditions and views selected to minimize skull reverberation artifacts while maximizing return echoes from internal brain structure.

In addition to the composite B-scan image, quantitative backscatter analysis employing the linear discriminant analysis of the tissue backscatter spectral

density function obtained from the A-mode waveform at selectable regions of the brain is available to improve the overall diagnostic capability of the instrument. Preliminary data suggest that at least four cerebral tissue types exhibit different spectral density functions<sup>22</sup> and thus with the visualization system would appear to add a new dimension to ultrasonic cerebral diagnosis.

### System Description and Operation

#### A. Patient Scanning

While more convenient and comfortable means were extensively examined for obtaining and maintaining adequate acoustic coupling, trapped air in the hair of patients requires that an immersion technique be used for scanning. The scheme used for this method is shown in Fig. 1, where the patient is supine and firmly supported on a positioning table which reclines approximately 30° to immerse the head in a warm (36° C), degassed, distilled water bath. The positioning system is automated so that the reclining movement is slow and smooth, with the head immersed to the brow. Trials with a number of subjects determined that during the examination period (10-15 minutes or less), minimal patient discomfort is experienced.

The low-frequency transducer mounted on the mechanical scan arm of the B-scan unit and immersed in the water bath is then manually moved in the desired anatomic imaging plane, while approximating orthogonality to the tangential plane at each scan point on the skull surface. The transducers are driven by a high-intensity pulser designed for the purpose of generating an acoustic pulse of an amplitude sufficient to overcome the approximate 20 dB round-trip loss at 1 MHz associated with attenuation in the skull. Details of the

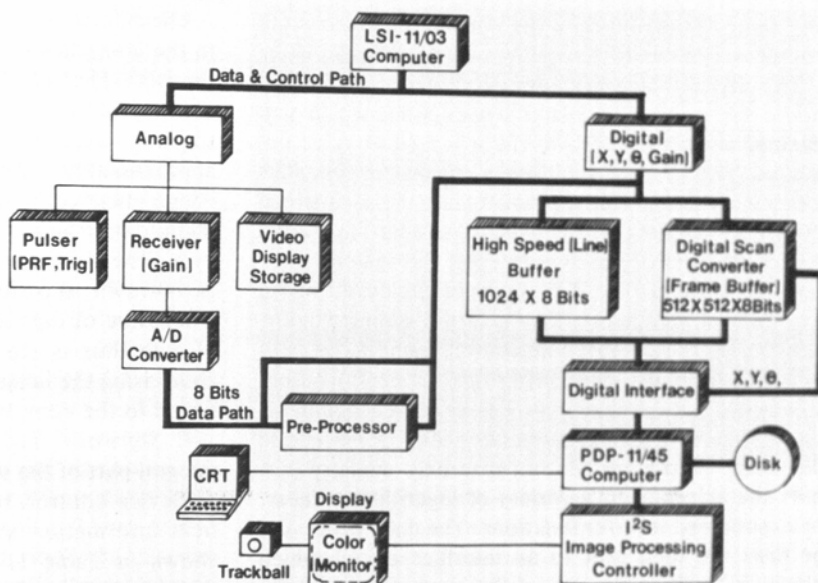


Fig. 2. Block diagram of ultrasonic transkull interrogation system hardware.

transducer and pulser design and assembly are available in a previous report.<sup>1</sup>

### B. Scan Unit and Signal Processing

1. *General.* The block diagram of the overall configuration of the UTIS system is shown in Fig. 2. The RF waveform obtained from the pulse-echo response of the transducer is received via the modified Searle system and sampled at a rate of approximately 8 MHz. The received RF data are passed through the digital peak detector (preprocessor) circuit and decimated for B-mode display. Also, these digital data are stored in the digital image controller (DIC), a  $512 \times 512 \times 8$  bit frame buffer interfaced to the PDP-11/45 computer. A library of programs (described fully later) is then available which allows the operator to transfer the image data as a file to a hard disk for permanent storage and further processing, while remaining immediately available for display on a high-resolution monitor via the image processing display. Here, the image processing library allows the operator to perform several interactive operations on the images to achieve an optimal amount of information concerning intracranial structure.

For interrogation for tissue classification using linear discriminant analysis of the A-mode spectral density function, the digitized RF and position data are stored on a  $1024 \times 8$  bit scratch pad memory (Interrogation Buffer) and transferred directly to the computer automatically upon operator request.

2. *Modified Searle B-scan Unit.* The greatly modified Searle Pho-Sonic® system has been described in detail previously<sup>1</sup> and will be treated only briefly here.

The instrumentation may be described in two parts: (a) the analog video system, including transducer, pulser, receiver, and associated circuitry, and (b) the digital video system, which includes the analog-to-digital converter, signal processing for longitudinal and lateral resolution optimization, and the interface with the commercial unit. The custom-built 750 kHz transducer (7.5-cm diameter lead metaniobate disc focused using an epoxy lens) has a focal distance of 22 cm and 3 dB lateral and longitudinal beam widths of 4.6 mm and 7.5 cm, respectively. A capacitive discharge pulser<sup>23</sup> is employed to drive the transducer to produce the acoustic pulse at an average acoustic power, via the radiation force method, of 35 mW (SPTA intensity  $150 \text{ mWcm}^{-2}$ ) under normal operation. This intensity is not unlike those reported for a wide range of commercial units.<sup>24</sup>

The received signals are then passed through an 82-dB variable high-voltage attenuator which regulates system gain and is linearly or logarithmically amplified with a respective dynamic range of 36 or 60 dB. The output of the receiver then is passed to the A/D converter, where a buffer provides an analog video output which may be used for external signal processing.

A logic system added to the commercial system allows switching from the normal commercial system operation to the transkull system, supplies PRF to the pulser and to the buffer, and provides an output from the machine for external signal processing. This logic also facilitates selection of log or linear amplification



and controls the routing of the signal through the depth compensation board.

The digital video system was designed to: (1) enhance longitudinal and lateral resolution, which was deemed inadequate due to the low frequency of operation, and (2) select various gain transfer functions and inject the transkull digital data into the commercial data train. RF data are digitized by an 8 bit Tektronix® ADC820T A/D digital converter at the system clock rate (8.74 MHz). The digital output is clocked into a longitudinal processor comprised of a sliding window (adjustable 1-16 point) comparator, found to be optimized at 6 points. The longitudinal processor output is clocked to the lateral processor which compares three lines of data to determine peaks in the lateral direction. A look-up table in read-only memory permits the selection of a variety of logarithmic, linear, or exponential transfer functions. The data (processed or raw) are then sent to an interface circuit which clocks it to the converter of the commercial unit for display.

**3. Image Processing.** The digitized RF waveforms are transferred to a PDP-11/45 computer for image processing via a two-stage interface, comprised of a digital image controller interface (DICI) and the digital image controller (DIC). The DICI performs two operations. First, it serves as a 1024×8 bit, high-speed line buffer for pulse-echo data to be read by the DIC. Second, it generates the pixel address for each data point by transforming the polar transducer position data to rectangular coordinates.

The DIC is a digital 512×512×8 bit, general-purpose frame buffer. An important feature of the DIC is an overwrite capability, which allows old data to be replaced by new data of greater intensity, useful when poor transducer alignment or anomalous attenuation inhibit the ability to obtain a satisfactory image from a single transducer scan. The inherent complexity of the DIC makes self-testing features a necessity. Therefore, a circuit which produces test patterns, including those which clear all pixels, gray scale, and checkerboard pattern and dot matrix, has been designed into the system.

The rate of data transfer from the B-mode scanner to the computer is staged at two speeds mediated by the DIC. The scanner digitizes its data at a 8.74 MHz rate for 400 μsec, in order to cover the tissue interrogation range of approximately 30 cm. This produces approximately 3333 bytes per line of data. Since the image plane contains 512 bytes of data per line maximum, data transfer could occur at about 2.5 μsec per byte. The maximum PDP-11/45 data acquisition rate is, however, too slow (50 μsec/byte) for transfer of a whole line of data at the PRF rate to occur. The line of data thus is stored in RAM, and when the lines comprising the image are all stored, the data are transferred to the computer at the slower rate.

**4. Software.** The computer program library is an integral part of the system, providing capabilities such as device control, testing, image processing, and patient information storage. Four major programs, as shown in Table 1, are currently available for these purposes and are denoted BRNVIS, TRAVIS, MASK, and INTBUF. BRNVIS mediates entry and display of patient identification and related information, scan coordinates, and plane orientation, as well as a number of image-affecting instrumentation variables, such as gain or transducer excitation, etc. Under TRAVIS, device selection, DIC and image processing, and data storage are controlled. Subroutines within this program control the read, write, and clear functions of the DIC and storage of selected images on a disk for later processing. Display command processing, display control, masking regions of particular interest, and the composition of artifact-free intracranial image are also accomplished with MASK.

**5. Tissue Classification.** The tissue interrogation aspect of the transkull system has been described previously,<sup>21,22</sup> and the analytic aspects of the classification scheme will only be briefly treated here. The scheme is based upon the hypothesis<sup>21</sup> that several of the tissue types within the brain exhibit characteristic backscatter spectra and that the backscatter spectra in the 0.5 to 1.5 MHz frequency interval can be used to classify brain tissue.

In the interrogation mode, A-mode data, 8 bits wide, from the linear amplifier prior to enhancement processing are sent to the computer, one line at a time, for later processing via the Interrogation Buffer Controller (IBC) previously shown in Fig. 2. The IBC operates in a FIFO manner, whereby data are clocked in from the A/D converter at a rate of 8.74 MHz and read by the PDP-11/45 under the INTBUF program. Along with analog signal data, transducer position data are stored in the buffer. This information is acquired from the LSI-11 computer on board the B-scan unit by the logic on the IBC and stored in the first four buffer positions. The position data are in vector format

Table 1. System Software for Control and Processing of Data

Program	Function
BRNVIS	Accept patient data
TRAVIS	Control DIC and Disk storage
MASK	Test DIC and image display
	Compose, display, and store images
INTBUF	Read and store A-mode data



$X_0$ ,  $Y_0$ ,  $X_r$ ,  $Y_r$ , where  $X_0$  and  $Y_0$  give initial position, and  $X_r$  and  $Y_r$  define the angle (ray angle =  $\tan^{-1}(Y_r/X_r)$ ). The current interrogation software requires 44 parallel A-mode scans to be taken at 1.5-mm intervals. To accomplish this in a reasonable time period, a feedback system has been developed to give position data via the computer terminal immediately back to the operator. With this system, a complete interrogative scan can be accomplished within 1 minute. The area of the scan is 190 mm deep by 66 mm wide. This means that approximately one-third of the brain cross section can be captured per scan.

The tissue characterization software separates each A-mode signal into five different frequency bands, located at 0.5, 0.7, 0.9, 1.1, and 1.3 MHz center frequencies. These data are squared and decimated to reduce the number of data points and then stored into five different files for further processing. These matrices are then normalized, passed through the classification algorithm,<sup>22</sup> and displayed on the Conrac® monitor. The classification algorithm then generates a sixth image, with the color of each pixel corresponding to the color assigned to the tissue classification for that case. Data resulting from these analyses have been described elsewhere.<sup>22</sup>

### C. Image Presentation

Images obtained with the UTIS system and the manner in which the composite images of the intracranial anatomy are constructed are shown in Fig. 3. The images are those of a 61-year-old male volunteer with assumed normal anatomy, at the HS60 horizontal scan plane.<sup>25</sup> In Fig. 3, A and B identify low-gain ultrasonic images of the left and right skull, respectively, and C and D identify the left and right brain hemispheres, respectively, taken at high ultrasonic gain. These component images are then digitally combined using MASK, and the scroll capability of the image processor forms the image presentation, denoted E, where the midline and other intracranial structures serve as landmarks. Ventricles and a variety of other anatomic brain features may be identified in these images. In addition to horizontal scans, coronal and sagittal views are also obtainable with this system.

In order to illustrate the type of structural details of brain anatomy and pathology visualized by the UTIS, transkull ultrasonic brain images of patients presenting intracranial pathology were compared with those obtained via x-ray computer tomography (CT). In these preliminary clinical studies, UTIS and x-ray CT scans were made of the same brain region for comparison. To date, two adult patients possessing previously diagnosed brain tumors (glioblastoma multiforme) have been available for such studies. Figure 4a is a com-

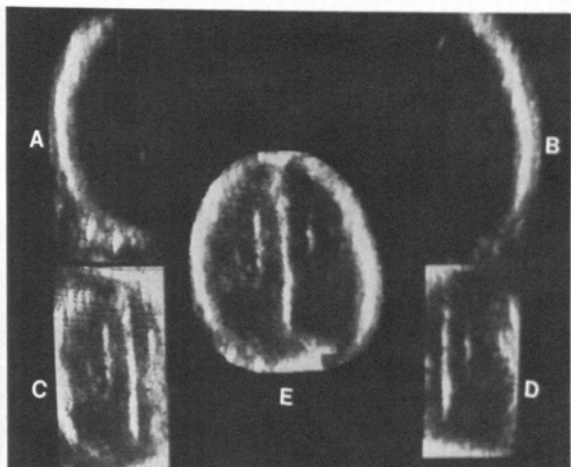


Fig. 3. Image reconstruction from component scan regions taken at selected gain settings (see text for explanation).

posite image, obtained with ultrasound transkull method, showing a drastic shift of the midline into the left hemisphere and prominent echo in the right hemisphere. The contrast-media-enhanced x-ray CT scan (Fig. 4b) also shows the midline shift and an x-ray dense region in the right hemisphere corresponding to the glioblastoma responsible for the distortion of the midline. Normalizing the scale of the two images (the ultrasound image is 10% smaller than that of the x-ray CT), it is seen that the x-ray dense region corresponds to that in the vicinity of the prominent echo in the right hemisphere obtained with ultrasound. Based upon internal skull measurements, the midline shift visualized via ultrasound is within 3% of that obtained

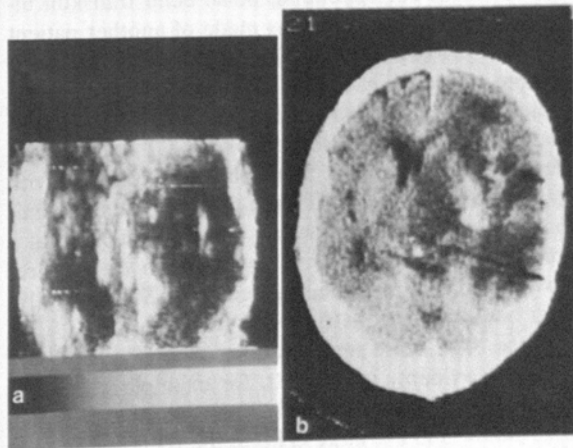


Fig. 4. (a) UTIS and (b) contrast-enhanced x-ray CT horizontal brain scans of approximately the same region with left hemisphere shown on left side of each image. Anterior is at the top, with midline shift due to presence of a glioblastoma multiforme evident in both images.

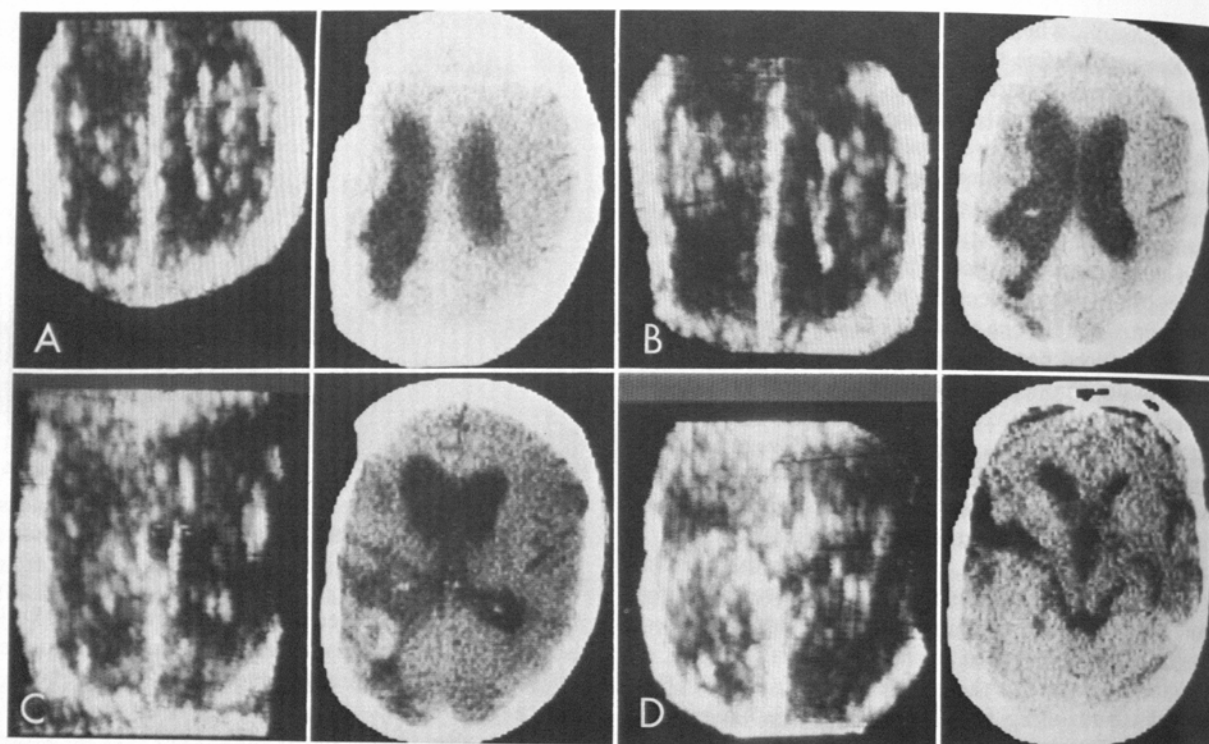


Fig. 5. Series of corresponding horizontal brain scans obtained via the UTIS (left) and contrast enhanced x-ray CT (right). Orientation is the same as in Fig. 4. Scans run in 1-cm successive increments from most cranial (A) to most caudal (D), ie, most cranial (A) and caudal 1 cm (B), 2 cm (C), and 3 cm (D) from position of (A). The tumor (glioblastoma multiforme) is clearly seen in (C) and (D) using both visualization techniques.

with x-ray CT, with the absolute difference between the two midline visualization techniques being approximately 0.7 mm.

A series of corresponding pulse echo transkull ultrasound and x-ray CT scans made of another patient is shown in Fig. 5, running from most cranial (Fig. 5A) to most caudal (Fig. 5D). This patient also possessed a glioblastoma but had been in remission for approximately ten years. The series of x-ray CT scans shows involvement of the left hemisphere posteriorly, with enlarged ventricles. Skull bone covering the left hemisphere is somewhat deformed since this subject, at a previous operation, had a large section of bone removed and not immediately repaired. Subsequently, skull bone was reconstructed in this region.

In the ultrasound series, a number of structural features are evident. In Fig. 5B, for example, the inter-hemispheric fissure is readily visualized via transkull ultrasound, and the large echo in the right hemisphere corresponds to the lateral border of the lateral ventricle. The ultrasound image in Fig. 5C shows clearly the lateral walls of the third ventricle and the most lateral aspect of the posterior portion. In Fig. 5D of the lateral

ventricle, the UTIS clearly visualized the tumor region. Transparent overlays show that the major tumor and ventricular regions were definable on the ultrasound scan and corresponded to those shown on the contrast-enhanced x-ray CT scan. In both cases examined thus far, however, x-ray CT displayed greater overall anatomic detail than UTIS, though these preliminary results are insufficient to fully judge the clinical diagnostic utility of the ultrasonic method. No clinical data have yet been collected using the tissue classification system, which could potentially enhance the imaging capability of the ultrasonic method and make the diagnosis more quantitative.

The brain regions most readily visualized with the UTIS appear to be in the horizontal plane from approximately 3 to 9 cm above the Frankfort plane. In coronal section from the lateral approach, the most easily visualized planes are from RA 2 to 3 cm to PA 6 cm, due predominantly to the nature of the internal and external surface aspects of the skull contour in those regions. Further clinical evaluation of the UTIS for patients presenting known intracranial diseases, as diagnosed by other methods, is yet required to ex-

amine the potential efficacy of the system for neuro-pathologic diagnosis.

### References

- Erdmann WA, Fry FJ, Johnston KW, Sanghvi NT. Instrumentation for ultrasonic transkull visualization. *IEEE Transactions on Sonics-Ultrasonics* 1982;SU-29:5-11.
- Dussik KT, Dussik F, Wyt L. Auf dem Wege zur Hyperphonographische des Gehirnes. *Medizinische Wochenschrift* 1947;97:425-429.
- Hueter TF, Bolt RH. An ultrasonic method for outlining the cerebral ventricles. *J Acoust Soc Am* 1951;23:160-167.
- Leksell L. Echo-encephalography I. Detection of intracranial complications following brain injury. *Acta Chir Scand* 1956;110:301-315.
- Leksell L. Echo-encephalography II. Midline echo from the pineal body as an index of pineal displacement. *Acta Chir Scand* 1958;115:255.
- deVlieger M, Ridder HJ. Use of echo-encephalography. *Neurology* 1959;9:216-223.
- deVlieger M, Molin CE, van der Ven C. Ultrasound for two-dimensional echo-encephalography. *Ultrasonics* 1963;1:148-151.
- Makow DM, Wyslouzil W, White DN, Blanchard J. Novel immersion scanner and display system for ultrasonic brain tomography. *Acta Radiol* 1966;5:855-864.
- Makow DM, McRae DL. Two-dimensional echo-encephalography using immersion scanning: recent results. In: Kazner E, Schiefer W, Zulch J (eds). *Proceedings in echo-encephalography*. New York: Springer-Verlag, 1968:197-201.
- Fry WJ. Intracranial anatomy visualized by ultrasound. *J Invest Radiol* 1968;3:243.
- Fry WJ, Leichner GH, Okuyama D, Fry FJ, Kelly E. Ultrasonic visualization system employing new scanning and presentation methods. *J Acoust Soc Am* 1968;44:1324.
- Fry FJ. Ultrasonic visualization of human brain structure. *J Invest Radiol* 1970;5:117.
- Heimburger RF, Fry FJ, Eggleton RC. Ultrasound visualization in human brain: the internal capsule. A preliminary report. *Surg Neurol* 1973;1:56.
- Fry FJ. Ultrasonic visualization of ultrasonically produced lesions in brain. *Confinia Neurologica* (Basel) 1970;32:38.
- Fry FJ. Ultrasonic surgical techniques. In: Richart RM, Prager DJ, Corfman PA, Van deWiele RL (eds). *Human sterilization*. Springfield: Charles C Thomas, 1972:160-165.
- Freund HJ, Somer JC, Dendel KH, Voight K. Electronic sector scanning in the diagnosis of cerebrovascular disease and space occupying processes. *Neurology* 1973;23:1147-1159.
- vonRamm OT, Smith SW, Kisslo JA. Ultrasound tomography of the adult brain. In: Lyons EA, White DN (eds). *Ultrasound in medicine*. Vol. 4. New York: Plenum, 1976:261-267.
- Fry FJ, Barger JE. Acoustical properties of the human skull. *J Acoust Soc Am* 1977;63:1576-1590.
- Fry FJ, Eggleton RC, Heimburger RF. Transkull visualization of brain using ultrasound: an experimental model study. In: deVlieger M, White DN, McCready VR (eds). *Ultrasonics in medicine* (Proceedings, 2nd World Congress on Ultrasound in Medicine). New York: Excerpta Medica/American Elsevier, 1974:97-103.
- Fry FJ. Transkull transmission of an intense focused ultrasonic beam. *Ultrasound Med Biol* 1977;3:179-184.
- Barger JE. Brain tissue classification by its ultrasonic backscatter. *IEEE Transactions on Sonics-Ultrasonics* 1981;SU-28:311-317.
- Barger JE, Campbell EJ, Chatigny JR. The classification of cerebral tissues by trans-skull ultrasonic interrogation. Bolt, Beranek & Newman, Inc., Report No. 4636, April 1981:1-28.
- Okyere JG, Cousin AJ. The design of a high voltage SCR pulse generator for ultrasonic pulse-echo applications. *Ultrasonics* 1979;17:81-84.
- Carson PL, Fischella PR, Oughton TV. Ultrasonic power and intensities produced by ultrasound equipment. *Ultrasound Med Biol* 1978;3:341-350.
- Delmas A, Pertuiset B. *Cranio-cerebral topometry in man*. Springfield: Charles C Thomas, 1959.